Analysis and simulation of a modified cardiac cell model gives accurate predictions of the dynamics of the original one

André H. Erhardt^a, Susanne Solem^b

^aWeierstrass Institute for Applied Analysis and Stochastics, Mohrenstraße 39, 10117 Berlin, Germany ^bDepartment of Mathematics, Norwegian University of Life Sciences, Norway

Abstract

The 19-dimensional TP06 cardiac muscle cell model is reduced to a 17-dimensional version, which satisfies the required conditions for performing an analysis of its dynamics by means of bifurcation theory. The reformulated model is shown to be a good approximation of the original one. As a consequence, one can extract fairly precise predictions of the behaviour of the original model from the bifurcation analysis of the modified model. Thus, the findings of bifurcations linked to complex dynamics in the modified model — like early afterdepolarisations (EADs), which can be precursors to cardiac death — predicts the occurrence of the same dynamics in the original model. It is shown that bifurcations linked to EADs in the modified model accurately predicts EADs in the original model at the single cell level. Finally, these bifurcations are linked to cardiac death at the tissue level by example.

Keywords: nonlinear dynamics, reaction-diffusion system, cardiac muscle cell, mathematical modelling 2010 MSC: 37G15, 37N25, 35Q92, 65P30, 92B05

1. Introduction

Mathematical modelling and simulations are important to investigate and analyse phenomena in life science. Two advantages of a detailed mathematical model is the possibility to use mathematical theory in order to get an in-depth understanding of the underlying mechanisms of certain dynamics, and to develop numerical experiments instead of real experiments. For instance, the mathematical models may be used for drug testing and to study drug response or its properties [1-6]. To derive a suitable mathematical model describing complex behaviour in biology like a cardiac action potential, based on experimental data, displaying all facets and dynamics of a cardiac muscle cell is a tough challenge. In addition to normal action potentials of a cardiac muscle cell, certain kinds of cardiac arrhythmia or chaos may occur [7-11]. This includes specific types of abnormal heart rhythms, which can lead to sudden cardiac death. It is therefore highly interesting and important to understand the complex behaviour and mechanism of such biological phenomena. A good mathematical model in combination with a meaningful analysis helps to decode these phenomena, the most prominent being early afterdepolarisations (EADs). However, due to the above mentioned multifaceted nature of cardiac cells, cardiac cell models can indeed be quite complex [12, 13]. This poses challenges both from a mathematical and computational point of view.

based on the TNNP04 model [15], is by now a well-established

The (endocardial) TP06 cardiac cell model [14], which is and much studied cardiac cell model [9–13, 16]. Despite that, a

rigorous mathematical analysis of all its dynamics is still lacking. Performing such an analysis on the model is hard due to two main things: the model is 19-dimensional and it is not smooth.

In this paper we modestly alter the non-smooth TP06 model in order to generate a smooth 17-dimensional version for which we can apply bifurcation theory. We show that the bifurcation theory aids in identifying complex dynamics linked to cardiac arrhythmia of the modified model, such as EADs. Through several examples, both at the single cell level and at the tissue level, we show that the bifurcation analysis of the modified model predicts similar, or even identical, dynamics of the original TP06 model. Thus, a bifurcation analysis of the modified model can help in decoding complex dynamics of the original model, which in turn can further the understanding of the heart.

Finally, we would like to emphasise that the approach in this paper can be utilised for other similar models stemming from the life sciences.

2. On modelling cardiac action potentials and related issues

The mathematical modelling of action potentials (APs) of excitable biological cells like neurons and cardiac muscle cells has its origin in the famous and pioneering Hodgkin-Huxley model [17]. Here, an approach was established that can be utilised to model APs of excitable biological cells by a system of ordinary differential equations (ODEs). In the last decades there has been an immense development in the modelling of cardiac muscle cells. These conductance-based models represent a minimal biophysical interpretation of an excitable biological cell in which current flow across the membrane is due to charging of the membrane capacitance and movement of ions across ion channels, which are selective for particular ionic species, cf. Figure 1. An initial stimulus activates the ion channels as soon as a certain threshold potential is reached. Then, these ion channels break open and/or up allowing an ion current flow, which changes the membrane potential. This elec-

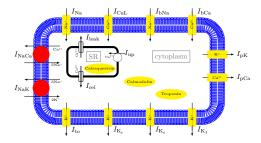


Figure 1: Scheme of a cardiac myocyte: SR denotes the sarcoplasmic reticulum, $I_{\text{NaCa}} = \text{Na}^+/\text{Ca}^{2+}$ a exchanger current & $I_{\text{NaK}} = \text{Na}^+/\text{K}^+$ a pump current [15].

trophysiological behaviour can be described by the following ODE using the Hodgkin–Huxley formalism:

$$C_m \frac{\mathrm{d}V}{\mathrm{d}t} = -I_{\text{ion}} + I_{\text{stim}}.\tag{1}$$

Here V denotes the voltage (in mV) and t the time (in ms), while $I_{\rm ion}$ is the sum of all transmembrane ionic currents. $I_{\rm stim} = 52~pA/pF$ (applied for 2 ms) represents the externally applied initial stimulus and $C_m = 1~\mu F/cm^2$ the membrane capacitance.

The main issue with several of the cardiac models of the form (1), from a mathematical point of view, is the requirement of a sufficiently smooth and regular ODE system in order to utilise theory such as bifurcation analysis. Bifurcation theory has already been widely utilised to investigate the dynamics of cardiac muscle cell models, see [18–26]. However, many of the existing detailed models are not smooth enough for the theory to be applied, see for example [27]. A second problem is that these systems may not exhibit a (suitable) equilibrium, i.e. the long-time behaviour $(t \to \infty)$ of the system does not converge into a stable steady state.

In addition, very detailed and high-dimensional models also cause numerical issues, as they might be quite sensitive and computationally expensive. This makes them harder to investigate. In general, lower-dimensional models are easier and faster to analyse and to simulate. However, important information can be lost. The desired aim of cardiac cell modelling is to study a most detailed cardiac muscle cell model, which simultaneously is mathematically and computationally feasible. To this end, we will focus on the 19-dimensional TP06 model [14], a cardiac model of the form (1) exhibiting the above mentioned issues: lack of smoothness, high-dimensionality, and lack of a computationally stable equilibrium. We will modestly reformulate the model in order to derive a good approximation and to be able to apply numerical bifurcation analysis using the CL_MATCONT, a continuation toolbox for MATLAB [28-30]. For this modified TP06 model symbolic derivatives up to the fifth order can be derived, which is desirable as it allows for discovering more complex bifurcations using the algorithm.

Although it is a modified TP06 model which is investigated using bifurcation theory in this paper, we will present several

examples validating that the analysis presented also provides fairly precise predictions of the dynamics of the TP06 model itself. As a first example, the two models produce indistinguishable output in the two plots in Figure 2. Figure 2(b) illustrates one example of an EAD. To be more precise, EADs are pathological voltage oscillations during the plateau or the repolarisation phase of the cardiac action potential and considered as potential precursors to cardiac arrhythmia.

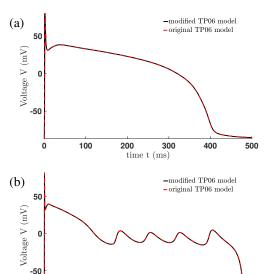


Figure 2: Comparison of the trajectories of the original TP06 model with the modified one. (a) normal action potential. (b) early afterdepolarisation. Here, we use $G_{\rm Cal}=0.000175~cm^3/(\mu Fs)$, cf. [15], to adjust the AP duration.

1000

time t (ms)

1500

2000

3. A reformulation of the TP06 model

500

The TP06 model contains several different ion currents, ion pump, ion exchanger and background currents:

$$I_{\text{ion}} = I_{\text{K1}} + I_{\text{to}} + I_{\text{Kr}} + I_{\text{Ks}} + I_{\text{CaL}} + I_{\text{NaK}} + I_{\text{Na}} + I_{\text{bNa}} + I_{\text{NaCa}} + I_{\text{bCa}} + I_{\text{pK}} + I_{\text{pCa}},$$

cf. [14, 15] and Figure 1. These currents are depending on individual ionic conductances $G_{\rm current}$ and Nernst potentials $E_{\rm current}$. Moreover, they may depend on gating variables, which are important for the activation and inactivation of the ion currents. For a full description of the variables involved, see [14]. The parameters used in this paper are the same as those in [14], with the exception of the $G_{\rm CaL}$ value, which is set to $G_{\rm CaL} = 0.000175 \ cm^3/(\mu F s)$.

The first smoothness issue is in the modelling of the sodium current in [14, 15], i.e.

$$I_{\text{Na}} = G_{\text{Na}} m^3 h \, j (V - E_{\text{Na}}),$$

where G_{Na} denotes the ionic conductance and E_{Na} the Nernst potential, while the different gating variables m, h and j satisfy

$$\frac{\mathrm{d}g}{\mathrm{d}t} = a_g(1-g) - b_g g = a_g - (a_g + b_g)g = \frac{g_\infty - g}{\tau_g},$$

where g represents the gating variables m, h and j, while $g_{\infty} := g_{\infty}(V) = a_g \cdot (a_g + b_g)^{-1}$ denotes the equilibrium of the gating variable g and $\tau_g := \tau_g(V) = (a_g + b_g)^{-1}$ its time scale. To be more precise, in the modelling of the gating variables h and j, the voltage dependent functions a_h , b_h , a_j and b_j are not continuous, cf. [15]. As the equilibrium of h and j are equal, we use the idea from [31] and reformulate h and h to one new gating variable h, and modify the sodium current to

$$I_{\text{Na}} = G_{\text{Na}} m^3 v^2 (V - E_{\text{Na}}).$$

Now, v satisfies the differential equation from above with $v_{\infty} = h_{\infty} = j_{\infty}$ and the time relaxation constant is given by

$$\tau_{v} = 0.25 + \frac{2.24 \cdot v_{\infty}}{(1 - \tanh(6.468 + 0.07 \cdot V))}.$$

As can be seen in the figures throughout the paper, this modification does not change the behaviour of the system dramatically. However, it is indeed a reformulation of the original TP06 model and the behaviours are not expected to be identical in all cases. Notably is also, regarding the bifurcation analysis, that we start with a steady state solution or equilibrium of the investigated system, i.e. $v_{\infty} = h_{\infty} = j_{\infty}$ is naturally satisfied.

A further problem is evoked by the modelling of the intracellular potassium ion concentration $[K]_i$. The modelling is the standard one, i.e.

$$\frac{d[K]_{i}}{dt} = -\frac{I_{K1} + I_{to} + I_{Kr} + I_{Ks} - 2I_{NaK} + I_{pK} + I_{stim}}{V_{c}F},$$

where V_c denotes the cytoplasmic volume and F the Faraday constant ($[K]_i$ is depending on the different potassium currents). For this equation it seems rather difficult or even impossible to find a steady state for which the continuation algorithm in CL_Matcont converges. To get around this issue, we removed this differential equation and set $[K]_i$ constant equal to the initial concentration $[K]_i$ of the TP06 model, $[K]_i = 138 \, mM$.

Comparing the resulting trajectories of both models, we see that they do not fit perfectly, cf. Figure 3. To balance

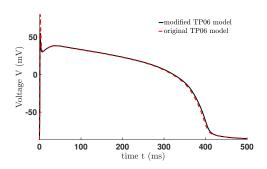


Figure 3: Comparison of the trajectories of the original TP06 model with the modified one with $I_{\rm stim}=52\frac{pA}{pE}$ applied for $2\ ms$.

this, we applied an external stimulus to our modified model of $I_{\text{stim}} = 71.5 \ pA/pF$ for 2 ms to produce Figure 2(a) and a slightly different one, $I_{\text{stim}} = 73.5 \ pA/pF$ for 2 ms, to gain Figure 2(b). Note that the trajectories are now identical. We

mention that the applied external stimulus affects the initial value/starting point of the system and it has an influence on the trajectory, cf. [32].

The advantage of these modest alterations of an already solid model is that we are now able to investigate complex dynamics by means of bifurcation analysis. We again like to stress that, as illustrated in the figures, the reformulated model is a fairly good approximation of the original one. Thus, we can to some extent extract from the analysis fairly precise predictions of the dynamics of the TP06 model [14].

4. Potassium dynamics of the modified model

In the previous section, we saw that replacing the ODE for the intracellular potassium ion concentration $[K]_i$ by $[K]_i \equiv 138 \ mM$ and the reformulation of the sodium current $I_{\rm Na}$, do not affect the dynamics of the modified model too much and can be at least compensated by a stronger external stimulus. To test potential limitations of this approach we now briefly study the potassium dynamics of the modified model.

To this end, we choose $[K]_i$ as bifurcation parameter and we start from $[K]_i = 138 \, mM$ to gain the bifurcation diagram in Figure 4. It contains a stable and unstable equilibrium branch

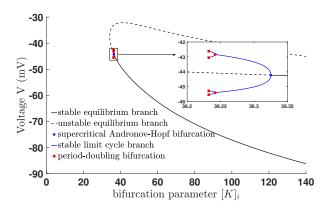


Figure 4: Potassium dynamics: Bifurcation diagram for the modified TP06 model with intracellular potassium ion concentration $[K]_i$ as bifurcation parameter (projection onto the $([K]_i, V)$ -plane).

(black solid and dashed line), respectively, and a supercritical Andronov–Hopf (AH) bifurcation (blue dot), from which a stable limit cycle branch (blue line) bifurcates. Furthermore, via a period doubling (PD) bifurcation (red square) the first limit cycle branch loses stability and a second stable limit cycle branch containing a second PD bifurcation bifurcates.

Starting from $[K]_i = 10 \ mM$ we get a second equilibrium branch with a second supercritical AH bifurcation, cf. Figure 5. Thus, the system exhibits two supercritical AH bifurcations, one for $[K]_i \approx 13.3562 \ mM$ and one for $[K]_i \approx 36.3252 \ mM$. From both AH bifurcations a stable limit cycle branch bifurcates. Indeed, the dominating dynamics are due to the one at $[K]_i \approx 13.3562 \ mM$ and its limit cycle branch, respectively.

Notice that both limit cycle branches collide with the unstable equilibrium branch and terminate there. In addition, it is obvious from Figure 5 that the modified TP06 model may exhibit

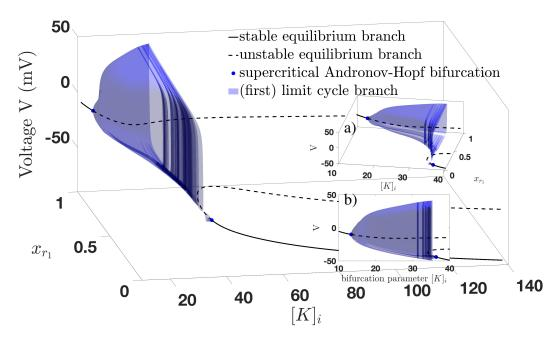


Figure 5: Potassium dynamics: Bifurcation diagram for the modified TP06 model with $[K]_i$ as bifurcation parameter including both AH bifurcation (projection onto the $([K]_i, x_{r_1}, V)$ -space). a) Zoom and rotation of the bifurcation diagram. b) Zoom and projection of the bifurcation diagram onto the $([K]_i, V)$ -plane.

periodic oscillatory pattern for a reduced intracellular potassium concentration $[K]_i$. Figure 5 also indicates that reducing $[K]_i$ at least determines whether the AP reaches it resting potential or not. For instance, $[K]_i = 40 \ mM$ implies that the trajectory has a stable equilibrium at approximately $-50 \ mV$. Therefore, the resting potential cannot be reached, cf. Figure 6.

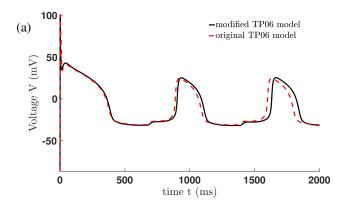
Comparing these findings with the original TP06 model by choosing the $[K]_i$ value of the modified TP06 model as the initial intracellular potassium concentration of the original TP06 model, we see that our bifurcation analysis yields also a fairly good predication for the dynamics of the original TP06 model, cf. Figure 6. More precisely, a reduction of the initial intracellular potassium concentration for the original TP06 model may lead to periodic oscillatory pattern.

This shows that fixing and varying $[K]_i$ leads to similar dynamics as changing the initial intracellular potassium concentration of the TP06 model. In both cases, the trajectories do not reach the resting potential and no further initial stimulus is needed to produce a change in the membrane potential, since periodic patterns occur, some sort of ventricular tachyarrhythmias [33–35]. Due to the fact that the resting phase is designated by high potassium currents, it is not surprising that the reduction of $[K]_i$ may inhibit the AP to reach its resting potential. Our analysis shows that considering a fixed intracellular potassium concentration is not a significant limitation and yields comparable results as in the TP06 model choosing the fixed $[K]_i$ value as initial value. The modification of the sodium current I_{Na} also modestly modify the behaviour of the system. Therefore, these modifications are reasonable and one can keep $[K]_i \equiv 138 \, mM$ fixed.

5. Reduction of the rapid and slow potassium currents

Due to the common knowledge that a reduction of the potassium currents, mainly the rapid one I_{K_r} , may lead to certain cardiac arrhythmia like EADs, it is natural to investigate the dynamics of the modified TP06 model by means of bifurcation analysis choosing one or more of the current specific conductances G_{K_r} and/or G_{K_s} as bifurcation parameter(s). Starting with the dynamics of the modified TP06 model with respect to G_{K_r} it turns out that the system has only for negative values of G_{K_r} an AH bifurcation and the limit cycle branch remains also on the negative part of the G_{K_r} -axis. Furthermore, no EADs (via a reduced rapid potassium current) appear, neither for the modified TP06 model nor for the original one, which corresponds also to the findings in [36]. However, EADs may appear via a reduced slow potassium current I_{K_s} and as a combination of a reduction of the fast and slow potassium currents. The potential effect of a reduced slow potassium current I_{K_s} is illustrated in Figure 7.

Therefore, we focus our study on the dynamics of the modified TP06 model with respect to a combination of $G_{\rm K_s}$ and $G_{\rm K_r}$. As one example for the occurrence of EADs via a combination of reduced $G_{\rm K_s}$ and $G_{\rm K_r}$, we consider a 75% blockade of the slow potassium current $I_{\rm K_s}$, i.e. $\bar{G}_{\rm K_s}=0.25\cdot G_{\rm K_s}$, and we choose the conductance $G_{\rm K_r}$ as bifurcation parameter, cf. Figure 8(a) & (b). Remember that our model is a 17 dimensional ODE system, thus we have a 17 dimensional phase space plus an additional dimension due to the bifurcation parameter. Therefore, the visualisation is tricky and we only present certain projections, which illustrate the dynamics well. In Figure 8(a) the equilibrium curve changes stability via a supercritical AH bifurcation (at $G_{\rm K_r} \approx -0.1120 \frac{nS}{pF}$) and a limit cycle branch bifurcates, which changes stability at a torus bifurcation (at



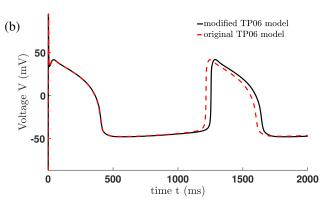


Figure 6: Comparison of the trajectories of the original TP06 model (initial value $[K]_i = 20 \text{ mM}$ or $[K]_i = 35 \text{ mM}$) with the modified TP06 model with $I_{\text{stim}} = 73 \frac{pA}{pF}$ applied for 2 ms and $[K]_i = 20 \text{ mM}$ (a) or $[K]_i = 35 \text{ mM}$ (b).

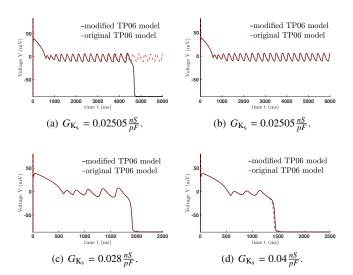


Figure 7: Comparison of the trajectories of the modified TP06 and the TP06 model with different reduced $G_{\rm K_s}$ value, where $G_{\rm K_r}=0.153~nS/pF$ is the value from [14]. Furthermore, in (b) - (d) a stimulus $I_{\rm stim}=71.5~pA/pF$ 7 over 2 ms was applied, while in (a) $I_{\rm stim}=73.5~pA/pF$ over 2 ms.

 $G_{\rm K_r} \approx -0.0623 \frac{nS}{pF}$), cf. [37], and exhibits a PD bifurcation (at $G_{\rm K_r} \approx -0.0119 \frac{nS}{pF}$). Notice that the AH bifurcation lies outside a physiological relevant range as well as the torus bifurcation and the PD bifurcations, cf. Figure 8(a). However, parts of the limit cycle branches are in a plausible range and determine the dynamics of the system. From the first PD bifurcation a further limit cycle branch bifurcates and contains a second PD bifurcation (at $G_{\rm K_r} \approx -0.0103 \frac{nS}{pF}$), where a third limit cycle branch bifurcates with a third PD bifurcation (at $G_{\rm K_r} \approx -0.0099 \frac{nS}{pF}$), cf. Figure 8(a). Such a PD cascade is an indication of the occurrence of EADs, cf. [18, 19, 32]. Although the analysis indicates that EADs appear, whether they actually do is also determined by the external stimulus.

This is visible in Figure 8(b), where we include only the first two limit cycle branches and consider only a physiological relevant range of G_{K_r} . Moreover, we include several trajectories of the modified system for different values of G_{K_r} (green lines).

Although, the autonomous system exhibits a PD cascade, EADs only appear if the trajectory of the non-autonomous ODE system can enter the inside of the (unstable) limit cycle branches and can surround the unstable equilibrium curve before leaving again the basin of attraction and reaching the resting potential. This indicates how initial values and/or the initial stimulus also decide whether a trajectory reaches a certain basin of attraction and certain dynamics appear. Finally, we want to highlight that the first trajectory in Figure 8(b), the one for $G_{K_r} = 0 \frac{nS}{pF}$, is the same trajectory as in Figure 2(b).

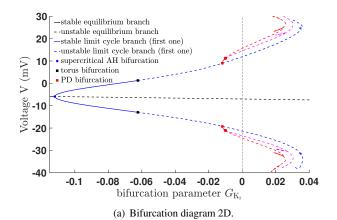
In addition, we investigate the effect of a blockade of both potassium currents by introducing a new parameter $\eta \in [0, 1]$:

$$\bar{G}_{K_r} = \eta \cdot G_{K_r}$$
 and $\bar{G}_{K_s} = \eta \cdot G_{K_s}$. (2)

This enables the study how a potential blockade of the fast and slow potassium current at the same time affects the dynamics of the modified TP06 model. This yields the bifurcation diagram in Figure 9 using η as bifurcation parameter reflecting the percentage of the blockade. Similar to Figure 8 the modified TP06 model exhibits a supercritical AH bifurcation for $\eta \approx 0.1628$, where a stable limit cycle branch bifurcates, which loses stability at a torus bifurcation ($\eta \approx 0.1645$) and from the first PD bifurcation ($\eta \approx 0.1971$) a second unstable limit cycle branch bifurcates. In this situation the dynamics of our interest, i.e. EADs, can be connected with the torus bifurcation (EADs with an extreme prolongation of the duration, but only for the modified TP06 model) and with the PD bifurcations (EADs with a "normal" prolongation of the duration for both models), cf. Figure 9(b) and Figure 10. We see that normal AP appears already as soon as the first limit cycle branch (with an unstable, repelling branch) covers the complex dynamics of the autonomous system. We also have in a physiologically relevant region a transition between an excitable and oscillatory media close to the supercritical AH bifurcation as in [32], cf. [38, 39].

6. Predictions of the modified model on the dynamics of the TP06 monodomain model

One major aim in cardiac research is to understand wave patterns like travelling waves, spiral waves, wave breakup and



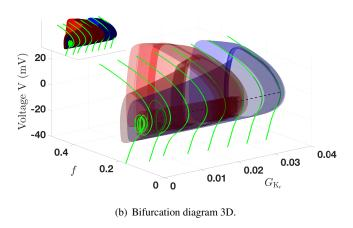


Figure 8: Bifurcation diagram of the modified model of [14] with a 75% blockade of the slow potassium current I_{K_s} , using G_{K_r} as bifurcation parameter: (a) Projection onto the (G_{K_r}, V) -plane. (b) Projection onto the (G_{K_r}, f, V) -space.

instabilities that might be linked to certain cardiac arrhythmia, see [38, 40–42]. In this section, we show by example that complex dynamics linked to EADs found through the bifurcation analysis of the modified model, yields complex dynamics on the tissue level of the TP06 model.

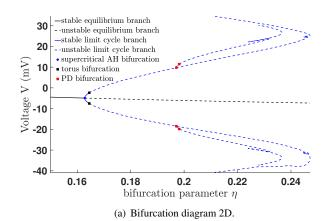
To study the behaviour of the model on macro-scale, we use the following 2D monodomain model:

$$C_m \frac{\partial V}{\partial t} = -I_{\text{ion}} + I_{\text{stim}} + \nabla \cdot \left(\begin{pmatrix} D & 0 \\ 0 & D \end{pmatrix} \nabla V \right), \tag{3}$$

where $C_m = 1 \mu F/cm^2$ and $D = 0.00154 cm^2/ms$, equipped with Neumann boundary condition. The diffusion matrix is chosen in accordance with [14]. Note that the mondomain model is directly linked to the bidomain model, which takes into account the anisotropy of the intra- and extracellular spaces. For a detailed description we refer to [43–48].

The simulations of the tissue level model (3) are run on a 1000×1000 grid with spatial discretization dx = 0.025 cm with a five-point stencil for the Laplacian (as in [10]) and with time step dt = 0.0812. The Rush and Larsen scheme [49] is used to integrate the gating variables in time, and Eulers method is used for the rest.

In Figure 11 we apply a stimulus of $I_{\text{stim}} = 26.2 \ pA/pF$ to



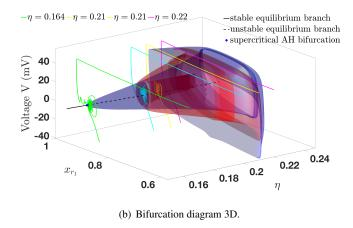


Figure 9: Bifurcation diagram of the modified model of [14] utilising η , cf. equation (2), as bifurcation parameter: (a) Projection onto the (η, V) -plane. (b) Projection onto the (η, x_{r_1}, V) -space.

 6×200 cells on the left side of the domain for both the normal parameter settings of the TP06 model and for the parameter settings in Figure 2(b).

The model (3) with the normal setting, presented in the left column, produces a wave that simply crosses the computational domain. In the beginning, system (3) with the other setting produces an identical wave to that of the one in the left column. Before t=600ms, however, this is no longer the case. After some time, the voltages at the top of the computational domain crosses the threshold (Figure 11(d)), which later results in similar voltage patterns to that of the fibrillation plots presented in [10]. Given that the parameter setting is within the range of EADs occurring for the modified model, this is to be expected for the original TP06 model.

Using a standard S1-S2 protocol to produce a spiral wave (see for example [10]) with the same initial stimulus as above and with normal parameter settings, we get the spiral wave depicted in Figure 12(a). Switching the parameters to that of Figure 2(b) after 4 seconds, which can be seen as a sudden onset of the effect of a drug, leads to cardiac death, see Figure 12(b)-(d).

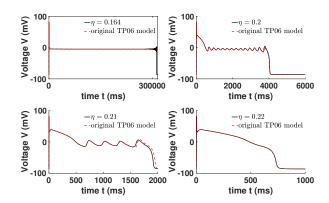


Figure 10: Trajectories of the modified TP06 model for different values of η , which are included in the bifurcation diagram 9(b).

7. Discussion and conclusion

The main focus of this paper is to better understand the TP06 model [14] through bifurcation analysis. This is done by a slight reformulation of the model, which is smooth and regular enough for bifurcation theory to be applicable. To this end we reformulated the sodium current I_{Na} and fixed the intracellular potassium concentration $[K]_i$ in the TP06 ODE system. This modification enables a proper mathematical analysis and a fairly good approximation of the TP06 model [14] by the modified one. As demonstrated, fixing the intracellular potassium concentration $[K]_i$ by the initial intracellular potassium concentration of the TP06 model [14] shows similar impact on the dynamics of both models. This finding was further validated by a detailed bifurcation analysis.

The bifurcation analysis of the modified TP06 model detected parameter values and ranges which induce EADs by a reduction of the rapid and slow potassium currents, $I_{\rm K_r}$ and $I_{\rm K_s}$, respectively. These findings indicate similar dynamics for the TP06 model [14], and that this is indeed the case was demonstrated through several examples for both the single-cell and monodomain TP06 model. Thus, the bifurcation analysis of the modified model can be used to predict dynamics in the TP06 model.

The modification does not give a perfect one-to-one relation between the two models, which is to be expected when one alters a model. It is however interesting that the modified model predicts the dynamics of the original TP06 model both for normal APs and EADs as well as it does.

Finally, we would like to point out that the bifurcation analysis encodes the behaviour of the underlying autonomous ODE system. However, the external stimulus and the initial values play a crucial role in whether certain dynamics actually occur or not. In fact, the stimulus determines whether the trajectory reaches the basin of attraction and if dynamics like EADs appear. Examining which dynamics actually do appear in a cardiac model is a general issue and the investigation of synchronisation is highly important due to the risk that the global heart's dynamics may shift the trajectory into a dangerous region.

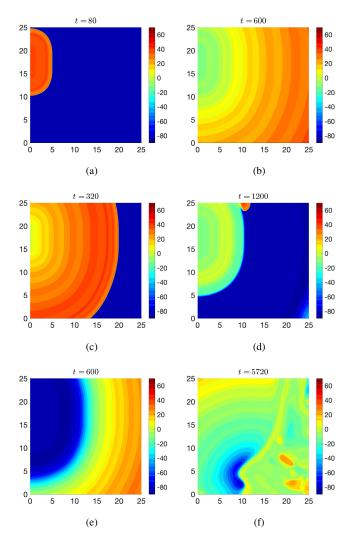


Figure 11: The monodomain model (3) is simulated by applying a 6×200 cells on the left side of the domain with the two parameter settings used to produce Figure 2. The time t is measured in milliseconds. The parameters of Figure 2(a) are used to produce the left column, and the parameters of Figure 2(b) are used to the right.

Conflict of interest. The authors declare no conflict of interest.

Acknowledgements. A.E., supported in 2020 by the Kristine Bonnevie scholarship 2020 of the Faculty of Mathematics and Natural Sciences, University of Oslo, during his research stay at Lund University, wishes to thank Erik Wahlén and the Centre of Mathematical Sciences, Lund University, Sweden for hosting him. Since March 2021, A.E. was supported by the DFG under Germany's Excellence Strategy – MATH⁺: The Berlin Mathematics Research Center (EXC-2046/1 – project ID: 390685689) via the project AA1-12*.

References

- [1] K. H. Jæger, V. Charwat, B. Charrez, H. Finsberg, M. M. Maleckar, S. Wall, K. E. Healy, A. Tveito, Improved computational identification of drug response using optical measurements of human stem cell derived cardiomyocytes in microphysiological systems, Frontiers in Pharmacology 10 (2020) 1648.
- [2] A. Tveito, M. M. Maleckar, G. T. Lines, Computing optimal properties of

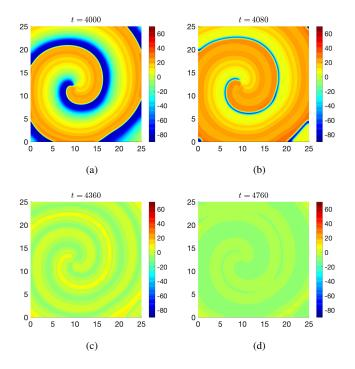


Figure 12: A spiral wave simulated with the monodomain model (3) with normal parameter settings. At t = 4s the parameter settings are switched to the ones used to produce Figure 2(b), leading to cardiac death. The time t is measured in milliseconds.

- drugs using mathematical models of single channel dynamics, Comput. Math. Biophys. $6\,(1)\,(2018)\,41-64.$
- [3] K. H. Jæger, S. Wall, A. Tveito, Detecting undetectables: Can conductances of action potential models be changed without appreciable change in the transmembrane potential?, Chaos 29 (7) (2019) 073102.
- [4] K. H. Jæger, S. Wall, A. Tveito, Computational prediction of drug response in short qt syndrome type 1 based on measurements of compound effect in stem cell-derived cardiomyocytes, PLOS Computational Biology 17 (2) (2021) 1–32.
- [5] F. Margara, Z. J. Wang, F. Levrero-Florencio, A. Santiago, M. Vázquez, A. Bueno-Orovio, B. Rodriguez, In-silico human electro-mechanical ventricular modelling and simulation for drug-induced pro-arrhythmia and inotropic risk assessment, Progress in Biophysics and Molecular Biology 159 (2021) 58–74.
- [6] X. Zhou, Y. Qu, E. Passini, A. Bueno-Orovio, Y. Liu, H. Vargas, B. Rodriguez, Blinded in silico drug trial reveals the minimum set of ion channels for torsades de pointes risk assessment, Front Pharmacol 10 (2020) 1643.
- [7] E. de Lange, Y. Xie, Z. Qu, Synchronization of early afterdepolarizations and arrhythmogenesis in heterogeneous cardiac tissue models, Biophysical Journal 103 (2) (2012) 365 373.
- [8] D. M. Roden, P. C. Viswanathan, Genetics of acquired long qt syndromeg, J. Clin. Invest. 115 (8) (2005) 2025–2032.
- [9] E. V. Nieuwenhuyse, G. Seemann, A. V. Panfilov, N. Vandersickel, Effects of early afterdepolarizations on excitation patterns in an accurate model of the human ventricles, PLoS ONE 12.
- [10] N. Vandersickel, I. V. Kazbanov, A. Nuitermans, L. D. Weise, R. Pandit, A. V. Panfilov, A study of early afterdepolarizations in a model for human ventricular tissue, PLoS ONE 9.
- [11] S. Zimik, N. Vandersickel, A. R. Nayak, A. V. Panfilov, R. Pandit, A comparative study of early afterdepolarization-mediated fibrillation in two mathematical models for human ventricular cells, PLoS ONE 10.
- [12] R. H. Clayton, O. Bernus, E. M. Cherry, H. Dierckx, F. H. Fenton, L. Mirabella, A. V. Panfilov, F. B. Sachse, G. Seemann, H. Zhang, Models of cardiac tissue electrophysiology: Progress, challenges and open questions, Prog. Biophys. Mol. Biol. 104 (1) (2011) 22 – 48.
- [13] M. Fink, S. A. Niederer, E. M. Cherry, F. H. Fenton, J. T. Koivumäki,

- G. Seemann, R. Thul, H. Zhang, F. B. Sachse, D. Beard, E. J. Crampin, N. P. Smith, Cardiac cell modelling: Observations from the heart of the cardiac physiome project, Prog. Biophys. Mol. Biol. 104 (1) (2011) 2 21
- [14] K. H. W. J. ten Tusscher, A. V. Panfilov, Alternans and spiral breakup in a human ventricular tissue model, Am. J. Physiol. Heart. Circ. Physiol. 291 (3) (2006) H1088–H1100.
- [15] K. ten Tusscher, D. Noble, P. J. Noble, A. V. Panfilov, A model for human ventricular tissue, Am. J. Physiol. Heart. Circ. Physiol. 286 (4) (2004) H1573–H1589.
- [16] J. Landaw, X. Yuan, P.-S. Chen, Z. Qu, The transient outward potassium current plays a key role in spiral wave breakup in ventricular tissue, American Journal of Physiology-Heart and Circulatory Physiology 320 (2) (2021) H826–H837.
- [17] A. L. Hodgkin, A. F. Huxley, A quantitative description of membrane current and its application to conduction and excitation in nerve, J. Physiol. 117 (4) (1952) 500–544.
- [18] A. H. Erhardt, Bifurcation analysis of a certain Hodgkin–Huxley model depending on multiple bifurcation parameters, Mathematics 6 (6) (2018) 1–15.
- [19] A. H. Erhardt, Early afterdepolarisations induced by an enhancement in the calcium current, Processes 7 (1) (2019) 1–16.
- [20] Y. Kurata, K. Tsumoto, K. Hayashi, I. Hisatome, M. Tanida, Y. Kuda, T. Shibamoto, Dynamical mechanisms of phase-2 early afterdepolarizations in human ventricular myocytes: insights from bifurcation analyses of two mathematical models, Am. J. Physiol. Heart. Circ. Physiol. 312 (1) (2017) H106–H127.
- [21] S. Otte, S. Berg, S. Luther, U. Parlitz, Bifurcations, chaos, and sensitivity to parameter variations in the sato cardiac cell model, Communications in Nonlinear Science and Numerical Simulation 37 (2016) 265–281.
- [22] D. X. Tran, D. Sato, A. Yochelis, J. N. Weiss, A. Garfinkel, Z. Qu, Bifurcation and chaos in a model of cardiac early afterdepolarizations, Phys. Rev. Lett. 102 (2009) 258103.
- [23] K. Tsumoto, Y. Kurata, K. Furutani, Y. Kurachi, Hysteretic dynamics of multi-stable early afterdepolarisations with repolarisation reserve attenuation: A potential dynamical mechanism for cardiac arrhythmias, Scientific Reports 7 (1) (2017) 10771.
- [24] M. E. G. Herrero, C. Kuehn, K. Tsaneva-Atanasova, Reduced models of cardiomyocytes excitability: comparing karma and fitzhugh-nagumo (2020). arXiv:2012.00804.
- [25] P. Rose, J.-H. Schleimer, S. Schreiber, Modifications of sodium channel voltage dependence induce arrhythmia-favouring dynamics of cardiac action potentials, PLOS ONE 15 (8) (2020) 1–14.
- [26] C. O. Diekman, N. Wei, Circadian rhythms of early afterdepolarizations and ventricular arrhythmias in a cardiomyocyte model, Biophysical Journal 120 (2) (2021) 319–333.
- [27] L. Priebe, D. J. Beuckelmann, Simulation study of cellular electric properties in heart failure, Circulation Research 82 (11) (1998) 1206–1223.
- [28] A. Dhooge, W. Govaerts, Y. A. Kuznetsov, Matcont: A matlab package for numerical bifurcation analysis of odes, ACM Trans. Math. Softw. 29 (2) (2003) 141–164.
- [29] A. Dhooge, W. Govaerts, Y. A. Kuznetsov, H. G. E. Meijer, B. Sautois, New features of the software matcont for bifurcation analysis of dynamical systems, Math. Comput. Model. Dyn. Syst. 14 (2) (2008) 147–175.
- [30] W. Govaerts, Y. A. Kuznetsov, A. Dhooge, Numerical continuation of bifurcations of limit cycles in matlab, SIAM J. Sci. Comput. 27 (1) (2005) 231–252.
- [31] O. Bernus, R. Wilders, C. W. Zemlin, H. Verschelde, A. V. Panfilov, A computationally efficient electrophysiological model of human ventricular cells, Am. J. Physiol. Heart. Circ. Physiol. 282 (6) (2002) H2296– H2308.
- [32] A. H. Erhardt, S. Solem, On complex dynamics in a purkinje and a ventricular cardiac cell model, Communications in Nonlinear Science and Numerical Simulation 93 (2021) 105511.
- [33] J. N. Weiss, A. Garfinkel, H. S. Karagueuzian, P.-S. Chen, Z. Qu, Early afterdepolarizations and cardiac arrhythmias, Heart Rhythm 7 (12) (2010) 1891 – 1899.
- [34] J. N. Weiss, Z. Qu, K. Shivkumar, Electrophysiology of hypokalemia and hyperkalemia, Circulation: Arrhythmia and Electrophysiology 10 (3) (2017) e004667.
- [35] J. Skogestad, J. M. Aronsen, Hypokalemia-induced arrhythmias and heart

- failure: New insights and implications for therapy, Frontiers in Physiology 9 (2018) 1500.
- [36] N. Vandersickel, E. Van Nieuwenhuyse, G. Seemann, A. V. Panfilov, Spatial patterns of excitation at tissue and whole organ level due to early afterdepolarizations, Frontiers in Physiology 8 (2017) 404.
- [37] A. H. Erhardt, K.-A. Mardal, J. E. Schreiner, Dynamics of a neuron-glia system: the occurrence of seizures and the influence of electroconvulsive stimuli, Journal of Computational Neuroscience 48 (2) (2020) 229–251.
- [38] B. Sandstede, A. Scheel, Spiral waves: linear and nonlinear theory (2021). arXiv:2002.10352.
- [39] S. Dodson, B. Sandstede, Determining the source of period-doubling instabilities in spiral waves, SIAM Journal on Applied Dynamical Systems 18 (4) (2019) 2202–2226.
- [40] S. Alonso, M. Bär, B. Echebarria, Nonlinear physics of electrical wave propagation in the heart: a review, Reports on Progress in Physics 79 (9) (2016) 096601.
- [41] E. M. Cherry, F. H. Fenton, T. Krogh-Madsen, S. Luther, U. Parlitz, Introduction to focus issue: Complex cardiac dynamics, Chaos: An Inter-disciplinary Journal of Nonlinear Science 27 (9) (2017) 093701.
- [42] A. Tveito, G. T. Lines, A condition for setting off ectopic waves in computational models of excitable cells, Mathematical Biosciences 213 (2) (2008) 141–150.
- [43] B. F. Nielsen, T. S. Ruud, G. T. Lines, A. Tveito, Optimal monodomain approximations of the bidomain equations, Appl. Math. Comput. 184 (2) (2007) 276–290.
- [44] J. Sundnes, G. T. Lines, B. F. Nielsen, K.-A. Mardal, A. Tveito, Computing the electrical activity in the heart, Springer, 2006.
- [45] A. Quarteroni, A. Manzoni, C. Vergara, The cardiovascular system: Mathematical modelling, numerical algorithms and clinical applications, Acta Numerica 26 (2017) 365–590.
- [46] A. Panfilov, H. Dierckx, V. Volpert, (invited) reaction-diffusion waves in cardiovascular diseases, Physica D: Nonlinear Phenomena 399 (2019) 1 – 34.
- [47] S. A. Niederer, J. Lumens, N. A. Trayanova, Computational models in cardiology, Nature Reviews Cardiology 16 (2) (2019) 100–111.
- [48] A. Tveito, K.-A. Mardal, M. E. Rognes (Eds.), Modeling Excitable Tissue, Springer International Publishing, 2021.
- [49] S. Rush, H. Larsen, A practical algorithm for solving dynamic membrane equations, IEEE Trans Biomed Eng 25 (1978) 389–392.